Mass-renormalized electronic excitations at $(\pi,0)$ in the superconducting state of $Bi_2Sr_2CaCu_2O_{8+\delta}$

A. D. Gromko,[1] A. V. Fedorov,[1,2] Y.-D. Chuang,[1,2] J. D. Koralek,[1] Y. Aiura,[3] Y. Yamaguchi,[3] K. Oka,[3] Yoichi Ando,[4] and D. S. Dessau[1]

[1]*Department of Physics, University of Colorado, Boulder, Colorado 80309-0390, USA*

[2]*Advanced Light Source, Lawrence Berkeley National Laboratory, Berkeley, California 94720, USA*

[3]*National Institute for Advanced Industrial Science and Technology (AIST), AIST Tsukuba Central 2, 1-1-1 Umezono, Tsukuba, Ibaraki 305-8568, Japan*

[4]*Central Research Institute of Electric Power Industry (CRIEPI), 2-11-1 Iwato-Kita, Komae, Tokyo 201-8511, Japan*

(Received 8 April 2003; published 17 November 2003)

Using high-resolution angle-resolved photoemission spectroscopy on $Bi_2Sr_2CaCu_2O_{8+\delta}$, we observe a new mass renormalization or ''kink'' in the E vs $\vec{k}$ dispersion relations localized near $(\pi,0)$. The resolution of bilayer splitting allowed the first direct measurements of this interaction effect. The kink is clearly stronger than the kink observed along the nodal direction, appears at a lower energy (near 40 meV for overdoped samples), and is only apparent in the superconducting state. The kink energy scale defines a cutoff below which well-defined quasiparticle excitations occur. The most likely origin of this effect is coupling to the magnetic-resonance mode observed in inelastic neutron scattering.

DOI: 10.1103/PhysRevB.68.174520 PACS number(s): 74.25.−q, 74.72.Hs, 78.70.Dm, 79.60.Bm

I. INTRODUCTION

A critical goal in the study of high-temperature superconductors (HTSCs) is an understanding of the interactions or correlation effects which ''dress'' the electrons near the Fermi energy E_F. This is important (1) for its own right, (2) because these interactions have been considered to be so extreme that even the concept of a quasiparticle may breakdown in these systems,[1,2] and (3) because any particularly strong interactions may serve as candidates for mediating the pairing of electrons within a Cooper pair, just as the interactions of the electrons with phonons is responsible for the pairing in conventional superconductors.

In the many-body language of solid-state physics, the electron self-energy $\Sigma(\vec{k},\omega)$ contains the information of these interactions or correlation effects. This dressing renormalizes the dispersion of electrons near the Fermi energy, giving them an enhanced mass or flatter E vs $\vec{k}$ dispersion. At large binding energies (greater than the energy of the boson being coupled to), the dispersion returns to its bare value, giving the dispersion a ''kink.'' The energy scale and strength of the kink are thus related to the boson energy and coupling strength, respectively.

In the HTSCs, particular attention should be payed to the electrons near the $(\pi,0)$ region of the Brillouin zone, which is the region in which both the ''nonquasiparticle like'' effects and superconducting pairing fluctuations are largest. In this paper, we present what we believe to be the first unambiguous evidence of mass renormalizations or kinks in the electronic structure near $(\pi,0)$ of a high-temperature superconductor. In particular, we used angle-resolved photoemission spectroscopy (ARPES) to make the first observations of a relatively low-energy kink of 40 meV or less (dependent on doping) which is distinct from the higher-energy (60-70 meV) kink which has been observed along the nodal or (π,π) direction of the Brillouin zone where the superconducting gap and other interaction effects are weakest.[3–7] In optimal and underdoped samples these energy scales merge and it is harder to deconvolve the two types of kinks.

Previous ARPES efforts at measuring kink or renormalization effects near the $(\pi,0)$ region have had great disparity. Lanzara[6] argued that the observed kink effects are essentially $\vec{k}$ independent, while Valla[4] and Kaminski[5] argued that the kink continually evolved, growing stronger as $(\pi,0)$ approached. Kaminski additionally argued that the kink at $(\pi,0)$ was the origin of the well-known peak-dip-hump (PDH) line shape.[9–11] We believe that the main reason for the disparity of these results was an inability to properly deconvolve the various features, especially the bilayer splitting. This deconvolution is especially difficult near $(\pi,0)$ as the features are numerous, overlapping, and typically quite broad. By overdoping high quality single-crystalline $Bi_2Sr_2CaCu_2O_{8+\delta}$ samples, we have obtained very sharp spectral features near $(\pi,0)$ and have been able to accurately deconvolve the bilayer splitting as well as superstructure effects[12,13] with similar work done by Feng *et al.*[14] and more recently, other studies as well.[15,16] This was a necessary prerequisite for this work. Our experiments give qualitatively different results than any of these previous studies, and additionally indicate that the PDH line shape previously observed near $(\pi,0)$[8–11] has major complications from the bilayer splitting, which obscures much of the true interaction effects. Other recent studies have indicated similar concerns of bilayer splitting on the PDH line shape.[15]

II. EXPERIMENTAL PARAMETERS

All measurements were performed at beam line 10.0.1 of the Advanced Light Source, Berkeley, and at beam line 5–4 of the Stanford Synchrotron Radiation Laboratory using SES 200 electron spectrometers. The experiments were done using 20-eV photons, with a combined experimental energy resolution of 12 meV, and a momentum resolution better than $0.01\pi/a$ (where a is the Bi2212 lattice constant) along the

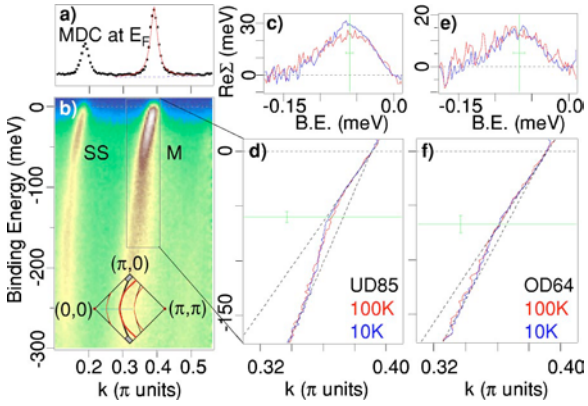

FIG. 1. (Color online) Nodal kink data as a function of doping (d),(f) and temperature (blue, red) from Bi2212. (b) shows raw data from a $T_c = 85$-K UD sample at $T = 10$ K. (a) Shows an MDC at E_F from these data (black dots) as well as a Lorentzian fit result (red lines). (d) and (f) show the centroids of these MDC fits at both 10 K (blue) and 100 K (red). (c) and (e) show ReΣ for both temperatures, as described in the text.

entrance slit to the spectrometer. We label our Bi2212 single crystals with a convention based on the transition temperature T_c, i.e., an overdoped (OD) Bi2212 sample with $T_c = 58$ K is referred to as OD58. The same convention is used for optimal (OP) and underdoped (UD) samples. All data were normalized to have the same intensity at a deep binding energy of about 400 meV, where the data are featureless [see, for example, Fig. 4(c)].

III. KINKS IN NODAL DATA

Figure 1(b) shows raw superconducting state data from a $T_c = 85$ K lightly underdoped sample (UD85) with the false color scale indicating the intensity of the features. We analyzed these data by taking momentum cuts at constant energy, otherwise known as momentum distribution curves (MDCs). Each MDC is made up of ≈ 90 data points, with a momentum resolution of better than $0.01\pi/a$ along the detector entrance slit. The MDC at the Fermi energy is plotted in panel (a), showing a fit to the main band peak consisting of a Lorentzian peak and linear background. This simple Lorentzian line shape is a product of the steep dispersion (or large dE/dk), and the relative independence of the electron self-energy as a function of momentum.[17] Panel (d) shows the MDC peak centroids between -175 meV and $+10$ meV, both above (red) and below (blue) T_c, extracted from Lorentzian fits. Panel (f) shows the same results from a $T_c = 64$ K overdoped sample (OD64). Following Johnson,[7] we use a straight line connecting the data between 0 meV and 175 meV to approximate the bare dispersion, i.e., the dispersion in the absence of the kink interaction. Note that this bare dispersion may contain additional interactions that make it different from the free-electron dispersion. Panels (c) and (e) show a subtraction of the experimental dispersion from the bare dispersion, for both temperatures on each sample. These plots show the energy difference between the two dispersions, ReΣ, as a function of binding energy. At both dopings we see that the temperature dependence of the kink interaction is a small effect compared to its strength in the normal state, an observation that helped Lanzara[6] to conclude that this peak was due to coupling to phonons. Consis-

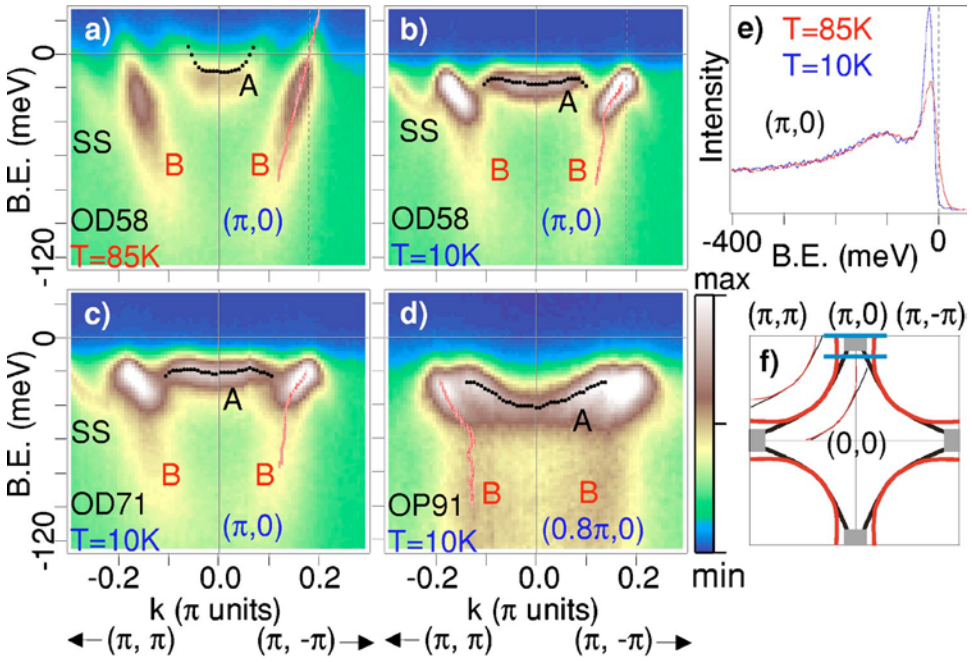

FIG. 2. (Color online) The ARPES dispersion kink near $(\pi,0)$. Panel (f) shows the Brillouin zone with bonding band B (red) and antibonding band A (black) Fermi surfaces, as well as cut locations for panels (a)–(d) (blue bars). The B band dispersions (red curves) were determined by fitting MDC peak positions. The black dots represent A band EDC peak positions. Panel (c) shows two representative EDCs at $(\pi,0)$ taken from panels (a) and (b).

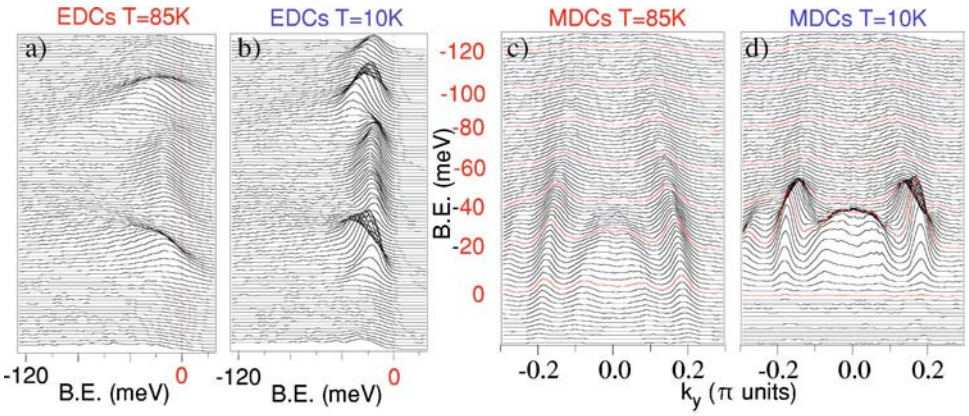

FIG. 3. (Color online) EDCs and MDCs at $T=10$ K and 85 K from the $(\pi,0)$ cut of sample OD58, from the data of Figs. 1(a) and 1(b).

tent with Johnson,[7] we observe a slight softening of the kink energy as the samples are underdoped. This doping dependence, which is extended to a wider range than the previous studies, is summarized by the red points in Fig. 7.

IV. KINKS AT $(\pi,0)$

Figures 2(a)–2(d) show raw data near the $(\pi,0)$ region [see panel (f)] taken on samples OD58, OD71, and OP91. In these curves the ARPES intensity is indicated by a linear color scale, as indicated by the color bar. The data of Figs. 2(a) and 2(b) are additionally shown in Fig. 3 in both EDC (energy distribution curve) form and MDC form. A salient feature of the data is the clear resolution of two bands, the higher-binding-energy bonding band (B) and the lower-binding-energy antibonding band (A), plus some weak superstructure bands due to the extra periodicity induced by the Bi-O plane lattice mismatch. Superimposed on top of the B band of Fig. 2 we show the peak positions (red) determined from Lorentzian fitting of MDCs, which are cuts in momentum space at constant energy.[18] Error bars from the fits are included, but are so small that they are essentially invisible. We also include the dispersion of the A band (black dots), extracted from the sharp low-energy peak in the EDCs.[19] A Lorentzian on a linear background was multiplied by a Fermi function. The normal-state B-band dispersion shown in panel (a) is seen to be nearly linear and featureless in the energy range displayed. Upon cooling the sample to 10 K [panel (b)], the dispersion as well as near-E_F spectral weight are radically changed. First, the features do not reach E_F because of the opening of the superconducting gap Δ. In addition to the gap opening, there is a clear kink in the dispersion around 40 meV. Although for samples OD71 and OP91 the spectral features are broader due to decreased doping [panels (c) and (d)], the data show a similar effect. Finally, the su-

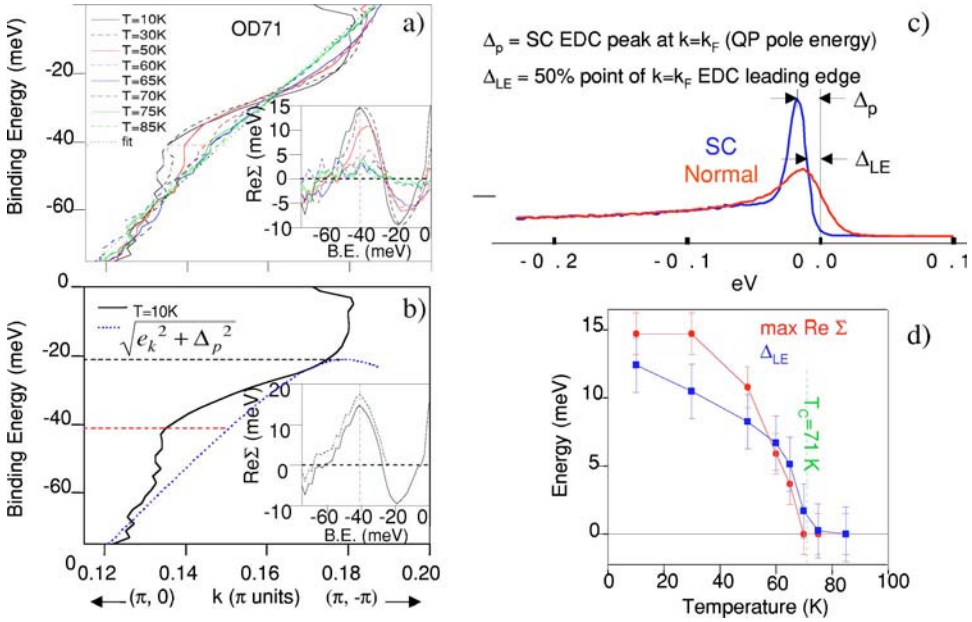

FIG. 4. (Color online) Temperature dependence of the $(\pi,0)$ kink strength. (a) MDC dispersion from OD71 along $(\pi,0)$-(π,π) [Fig. 2, panel (c)]. The inset shows the temperature dependence of ReΣ determined using a linear fit to the dispersion (see text). The kink energy is $\approx$40 meV. (b) $T=10$-K MDC dispersion (solid black) compared to the expected Bogoliubov dispersion (blue dots) using the measured gap Δ_p [panel (c)] and $T=85$-K dispersion [panel (a)], as described in the text. The inset compares ReΣ from this method (dotted line) to that of panel (a) (solid line). (d) Temperature dependence of the maximum in ReΣ (red circles) from panel (a) and the superconducting gap $\Delta_{LE}(T)$ (blue squares).

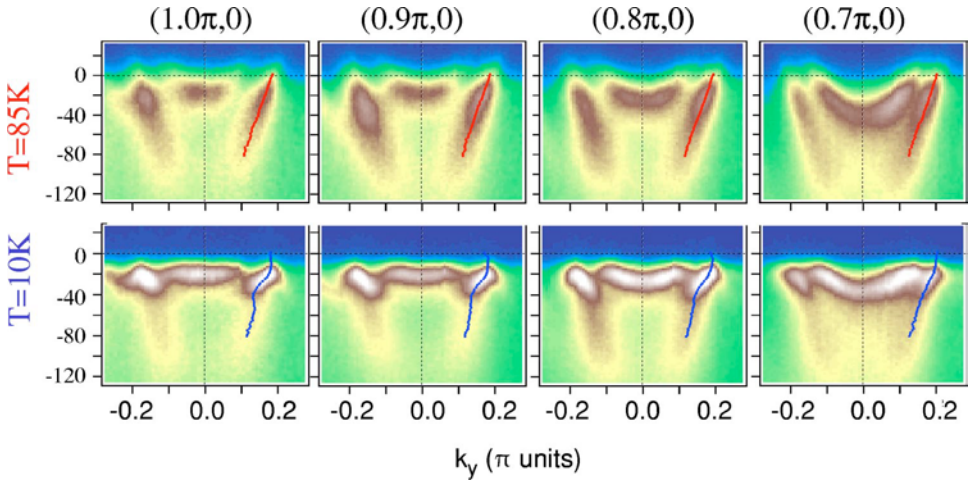

FIG. 5. (Color online) k dependence of the kink strength, for sample OD71, at $T=85$ K (top) and 10 K (bottom). MDC-derived dispersions for the positive k_y (superstructure-free) side B band dispersion are overlaid in red and blue.

perconducting state ARPES peaks are seen to be sharp and intense for binding energies below the kink energy, whereas they are more strongly damped for binding energies above the kink energy, as well as for all energies in the normal state as observed in previous ARPES data.[5,11,20]

V. TEMPERATURE AND MOMENTUM DEPENDENCES

The temperature dependence of the $(\pi,0)$ kink can be seen in Fig. 4(a), where the MDC-derived bonding band dispersion from sample OD71 [Fig. 2(c)] is shown at a series of temperatures taken on cooling through T_c. The black dotted line is a linear fit to the highest temperature ($T=85$ K) data. Since this dispersion is featureless, it appears that whatever interaction is responsible for the 40-meV kink is essentially absent in the normal state, i.e., we can consider this the noninteracting dispersion for this effect. Other interactions that modify the normal-state dispersion are of course likely to be present as well—for example the roughly factor of 2 decreased dispersion that is observed compared to the local-density approximation dispersion.[21] The component of the self-energy that is discussed here ignores any self-energy effects that modify the normal state.

To highlight the temperature-dependent effects we subtract the superconducting state MDC dispersion from the normal-state dispersion, shown in the inset to panel (a), giving an experimental estimate of ReΣ. An artifact of the MDC analysis is that inside the gap region (≈ 0 -25 meV), where there is no real quasiparticle peak, the MDC method finds a peak due to the finite-energy width of the spectra. We thus focus on the energy range between 25 and 75 meV.

An alternative way to extract ReΣ in the superconducting state is to compare the measured dispersion to that expected with the opening of a superconducting gap. This is illustrated in panel (b). The dotted curve is the expected superconducting (SC) state "Bogoliubov" quasiparticle dispersion computed from the measured normal-state dispersion e_k [Fig. 4(a)] and the measured low-temperature gap Δ_p, obtained from the peak position of the EDC measured at k_F [see panel (c)]. On top of this we plot the measured low-temperature dispersion (solid black), [also plotted in panel (a)], which clearly deviates strongly from the expected SC state dispersion. The difference is plotted in the inset to panel (b) as the dotted curve. The black curve in the inset is extracted from the inset of panel (a). While this method probably produces a slightly more accurate estimate of ReΣ than that in the inset to panel (a), it is more difficult to apply at elevated temperatures where the thermal broadening becomes comparable to Δ_p and additional fittings are necessary to extract these parameters. The general similarities of the two curves in the panel (b) inset does indicate that the extraction of panel (a) is an adequate estimate of ReΣ.

Panel (d) shows the maximum point of each ReΣ curve from the inset in panel (a) as a function of temperature (red),

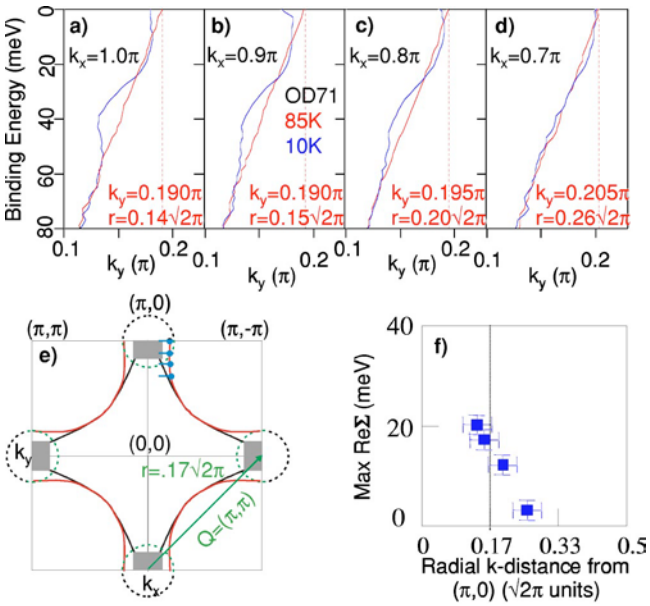

FIG. 6. (Color online) k dependence of the kink strength, part 2. (a)–(d) MDC-derived B-band dispersion from sample OD71 (raw data from Fig. 5). The red dashed lines mark the FS crossings, which are labeled on each panel along with the radial distance from $(\pi,0)$. (e) A schematic of the 2D Fermi surface. The INS wave vector (green) naturally connects the $(\pi,0)$ and $(0,\pi)$ points and has half-intensity points which roughly map to the green circles. (f) The kink strength as a function of the radial distance from the $(\pi,0)$ point. The node occurs at 0.5.

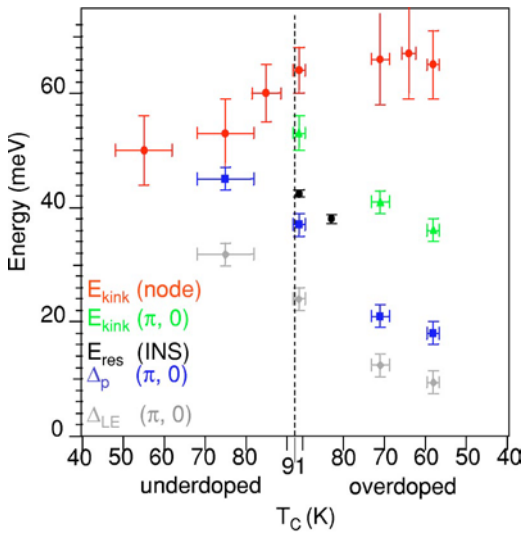

FIG. 7. (Color online) Summary of the doping dependence of the energy scales of the ARPES kinks, gaps, and the INS resonance, for both underdoped (left) and overdoped (right) samples. E_{kink} (node) is from our own unpublished data and E_{res} (INS) is from He *et al.*[28]

which is seen to have an onset at or very near $T_c = 71$ K. In addition, we also plot the superconducting gap Δ_{LE} as a function of temperature (blue) extracted from the identical dataset by simply measuring the shift of the midpoint of the EDC leading edge from E_F. Here we plot $\Delta_{LE}(T)$ in lieu of the gap $\Delta_p(T)$, determined from EDC peak positions, because a reliable determination of $\Delta_p(T)$ is made difficult by thermal broadening for T near T_c. We see that the maximum in $\mathrm{Re}\Sigma$, which provides a measure of the coupling strength, tracks the opening of the superconducting gap, making it clear that the two are closely related.

Figures 5 and 6 show the $\vec{k}$ dependence of the ARPES kink, measured on sample OD71. We show data along four-momentum slices centered around the $\vec{k}$ values of $(\pi,0)$, $(0.9\pi,0)$, $(0.8\pi,0)$, and $(0.7\pi,0)$. Raw data as well as MDC peaks from Lorentzian fitting are shown in Fig. 5, with the results summarized in Figs. 6(a–d). From the progression we see that the kink energy stays approximately the same throughout this *k*-space region. Its intensity, however, weakens dramatically as we move away from the $(\pi,0)$ point, such that it is barely visible in the 0.7π cut of panel (d). This falloff in kink strength is shown in panel (f), which shows the intensity of the kink [plotted as $\mathrm{Re}(\Sigma)$] as a function of radial position from the $(\pi,0)$ point.

VI. DOPING DEPENDENCES AND ENERGY SCALES

Figure 7 summarizes the energy scales of the nodal kink (red circles), the $(\pi,0)$ kink (green triangles), as well as a number of other phenomena over a wide range of doping levels. It is clear from these data that the two kinks occur at different energy scales and have different doping dependences. Near optimal doping where most previous kink studies were done, the energy scales of the two kinks merge (Fig. 7), making it much more difficult to deconvolve the difference in the scales.

VII. ORIGIN OF THE $(\pi,0)$ KINK

From the above data, the differences between the $(\pi,0)$ kink and the well-studied nodal kink can be summarized as follows.

(1) The $(\pi,0)$ kink strength is strongly temperature dependent and is observed only below T_c [Fig. 4(d)], while the nodal kink is observed above T_c as well.[8]

(2) The $(\pi,0)$ kink is at a significantly lower energy scale than the nodal kink (Fig. 7) and has a different momentum and doping dependence.

(3) The strength of the $(\pi,0)$ kink (or coupling strength) is much stronger than the nodal kink.[22] These points make a strong case that the two kinks are *separate entities* arising from *different phenomena*.

Because the $(\pi,0)$ kink occurs in the region of the Brillouin zone where the superconducting gap and pairing correlations are the strongest, as well as the fact that the effect only occurs in the superconducting state, it is especially important to understand its origin. It may even be that the mechanism which causes this kink plays a very strong role in the superconductivity. The following paragraphs thus discuss a number of possible scenarios for the origin of the $(\pi,0)$ kink, though more are likely to surface as well. This part of the paper is, necessarily, more speculative than the previous portion which presented the direct experimental data.

The two main classes of explanations that we are aware of are (1) a byproduct of the opening of the superconducting gap and (2) a strong coupling to a bosonic excitation such as a phonon or collective magnetic excitation.

In the first class of explanations we consider the damping of the system (peak broadening) to be due principally to electron-hole excitations. In the superconducting state each branch (the initial electron plus the excited electron-hole pair) will see a turn on at the gap energy Δ, leading to a step in the damping rate $\mathrm{Im}\Sigma$ near an energy 3Δ.[23] This will in turn introduce structure into $\mathrm{Re}\Sigma$ (as seen by a Kramers-Krönig analysis), and could be imagined as the origin of the kink. However, an important problem with this picture is that as the temperature is raised towards T_c, the energy of the kink is observed to decrease slowly, staying at a sizable finite value [Fig. 4(a)]. In contrast, the 3Δ model would predict that the kink energy should decrease to zero at T_c, just as Δ does. We note that while in UD samples the gap may remain finite up to and across T_c, the gap clearly does decrease to zero or near zero at T_c in these OD samples [Fig. 4(d)].

Electron-phonon coupling is the most well-known and simplest example of the second class of explanations, coupling to a bosonic excitation. In general, we do not expect electron-phonon coupling strengths to vary greatly with temperature because the phonons are present equally above and below T_c. Also, because the coupling is typically mostly local in nature, we do not expect the mass-renormalization effects due to electron-phonon coupling effects to be strongly *k* dependent. Therefore, the very strong temperature dependence of the $(\pi,0)$ kink, as well as the tight localization of the kink in *k* space make it unlikely that electron-phonon coupling is responsible for this effect. It does however, remain a possibility for the nodal kink, as proposed recently by

Lanzara.[6] Another possibility for the origin of the nodal kink is coupling to the local magnetic susceptibility, which is observed in $\vec{Q}$ integrated INS measurements and which occurs with a slightly higher energy than the magnetic-resonance mode.[24]

VIII. COUPLING TO THE MAGNETIC-RESONANCE MODE

The prime candidate for a bosonic excitation is the magnetic-resonance mode observed in inelastic neutron scattering (INS) experiments. This mode only occurs below T_c,[25] or in underdoped samples below T^*,[26] making the turn on of the effects we see at T_c very natural. Previously, it had been proposed that the INS magnetic resonance manifests itself in the ARPES EDC line shape, primarily as the origin of the ''classic'' PDH line shape,[5,11,20] though it is now clear that the bilayer splitting causes a major complication to these interpretations, with it even possible that much of the classic PDH effect is simply due to the existence of the bilayer-split bands.[22,27] In momentum space, the mode has a Q vector (momentum transfer) centered at (π,π), which naturally connects the k regions $(\pi,0)$ and $(0,\pi)$ where the kink effect is most strongly seen. This is schematically illustrated in Fig. 6(e). The resonance mode intensity as a function of momentum transfer $\vec{Q}$ has been measured on an OD83 Bi2212 sample by He *et al.*[28] They found that the mode intensity is peaked at $\vec{Q}=(\pi,\pi)$ and has its half-intensity points at $\approx\vec{Q}=0.67(\pi,\pi)$ and $1.33(\pi,\pi)$ along this cut. Other neutron measurements indicate that the mode falloff is roughly isotropic in $\vec{Q}$ space.[29] We show these half-intensity points schematically on the Brillouin zone in panel (e) as green circles centered around $(\pi,0)$ and $(0,\pi)$, according to the standard belief that the (π,π) mode connects these points since they have the largest near-E_F electron density and are separated by a vector of (π,π).[20,30,31] The circles are drawn with a radius of $0.17\sqrt{2}\pi$ so that the closest (furthest) edges are connected by a $\vec{Q}$ of $0.67(\pi,\pi)$ and $[1.33(\pi,\pi)]$.

We converted the $\vec{k}$-space values of the Fermi-surface crossings into a radial $\vec{k}$ distance from the $(\pi,0)$ points in units of $\sqrt{2}\pi$, listed in panels (a)–(d) of Fig. 6. In these units the $(\pi,0)$ point occurs at 0 and 1.0 and the node occurs near 0.5. ReΣ from panels (a)–(d), obtained using the method of Fig. 4(a), are plotted versus radial distance from $(\pi,0)$ in panel (f). We see that the line at $0.17\sqrt{2}\pi$ corresponding to the green circles in panel (e) occurs near the half intensity of where ReΣ would extrapolate at $(\pi,0)$. Therefore, the falloff in intensity of ReΣ as a function of $\vec{k}$ is in very good first-order agreement with what is expected from the falloff in intensity of the INS mode as a function of $\vec{Q}$. This makes an intimate relationship between the kink and the magnetic mode highly plausible. Recent theoretical work also supports this view.[34]

In addition to considering the temperature and momentum dependence of the $(\pi,0)$ kink, we should consider its energy scale as well. The mode has a characteristic energy near ''41 meV,'' though this energy scale is actually doping dependent with decreasing energy scales as the samples are progressively overdoped. This effect is shown by the black circles in Fig. 7, from He *et al.*[28] Also shown on this plot are the low-temperature superconducting gap values measured from the $(\pi,0)$ datasets of this paper, including two methods of gap determination, Δ_p (blue squares) and Δ_{LE} (gray diamonds) [Fig. 4(c)].

Following the analogy of $\alpha^2F(\omega)$ oscillations in strongly electron-phonon coupled conventional s-wave superconductors, we may expect the $(\pi,0)$ kink to be observed at an energy equal to $\Delta+\omega_R$, where Δ is the superconducting gap and ω_R is the neutron-resonance mode energy.[20,32] If we choose the superconducting state EDC peak position Δ_p at $(\pi,0)$, the energies $\Delta_p+\omega_R$ will clearly be larger than the kink energy scale, though if we choose the leading edge half-maximum point Δ_{LE} at $(\pi,0)$, the agreement between $\Delta_{LE}+\omega_R$ and the kink energy scale is much better. Regardless of whether this should be considered an agreement of energy scales, it is not surprising that the situation should be more complicated in the cuprates than in conventional superconductors. For one, the resonance mode to which the electrons appear to be coupling is not yet understood, even at the basic level of whether it corresponds to particle-particle[33] or particle-hole[20,32] excitations. Also, since the magnetic mode is electronic in origin and only occurs in the paired state, there is a likelihood of a strong feedback effect that may change the observed energy scale. Finally, we note that the strong coupling near the $(\pi,0)$ point makes vertex corrections much more important,[35] and these as well as possible excitonic effects[32] may lower the energy of the kink. Additionally, possible bosonic excitations which may couple to the $(\pi,0)$ electrons could be considered, including, for example a mode in the charge channel.

IX. SUMMARY

We have made detailed measurements on Bi2212 which delineate mass-renormalization or ''kink'' effects near $(\pi,0)$ from those near the node, and we find significant differences between the two. While the nodal kinks are observed both above and below T_c and have only a weak temperature dependence, the $(\pi,0)$ kink is observed only below T_c and has a very strong temperature dependence. In the overdoped regime the two effects also have a significantly different energy scale [near 40 meV for the $(\pi,0)$ kink and 70 meV for the nodal kink] though the two scales merge together near optimal doping. The strength of the $(\pi,0)$ kink decreases rapidly away from $(\pi,0)$. While the nodal kink may be due to coupling to phonons as previously argued, the $(\pi,0)$ kink is inconsistent with this possibility and is most likely due to coupling to an electronic excitation. In particular, the INS magnetic-resonance mode is attractive as an origin of the effect because the $\vec{k}$ dependence of the kink intensity away from $(\pi,0)$ is similar to what is expected from the $\vec{Q}$ dependence of the INS magnetic-resonance mode intensity.

Note added. Recent experimental work by Kim *et al.* has observed a $(\pi,0)$ kink in Pb-Bi2212.[36]

ACKNOWLEDGMENTS

We acknowledge beam line support from X. J. Zhou, P. Bogdanov, Z. Hussain, and D. H. Liu, and helpful discussions with G. Blumberg, A. Chubukov, C. Kendziora, A. Millis, P. Lee, D. Pines, D. Scalapino, J. Schmallian, Z-X. Shen, and S. C. Zhang. We gratefully acknowledge the help of R. Goldfarb at NIST for the use of the SQUID magnetometer. Support is from NSF Career Grant No. DMR-9985492 and DOE Grant No. DE-FG03-00ER45809. ALS and SSRL are operated by the DOE, Office of Basic Energy Sciences.

[1] P.W. Anderson, *The Theory of Superconductivity in the High-T_c Cuprates*, Princeton Series in Physics (Princeton University Press, Princeton, NJ, 1997).

[2] C.M. Varma, P.B. Littlewood, S. Schmitt-Rink, E. Abrahams, and A.E. Ruckenstein, Phys. Rev. Lett. **63**, 1996 (1989).

[3] P.V. Bogdanov, A. Lanzara, S.A. Kellar, X.J. Zhou, E.D. Lu, W.J. Zheng, G. Gu, J.-I. Shimoyama, K. Kishio, H. Ikeda, R. Yoshizaki, Z. Hussain, and Z.X. Shen, Phys. Rev. Lett. **85**, 2581 (2000).

[4] T. Valla, A.V. Fedorov, P.D. Johnson, Q. Li, G.D. Gu, and N. Koshizuka, Phys. Rev. Lett. **85**, 828 (2000).

[5] A. Kaminski, M. Randeria, J.C. Campuzano, M.R. Norman, H. Fretwell, J. Mesot, T. Sato, T. Takahashi, and K. Kadowaki, Phys. Rev. Lett. **86**, 1070 (2001).

[6] A. Lanzara, P.V. Bogdanov, X.J. Zhou, S.A. Kellar, D.L. Feng, E.D. Lu, T. Yoshida, H. Eisaki, A. Fujimori, K. Kishio, J.-I. Shimoyama, T. Noda, S. Uchida, Z. Hussain, and Z.-X. Shen, Nature (London) **412**, 510 (2001).

[7] P.D. Johnson, T. Valla, A.V. Fedorov, Z. Yusof, B.O. Wells, Q. Li, A.R. Moodenbaugh, G.D. Gu, N. Koshizuka, C. Kendziora, Sha Jian, and D.G. Hinks, Phys. Rev. Lett. **87**, 177007 (2001).

[8] D.S. Dessau, B.O. Wells, Z.X. Shen, W.E. Spicer, A.J. Arko, R.S. List, D.B. Mitzi, and A. Kapitulnik, Phys. Rev. Lett. **66**, 2160 (1991).

[9] D.S. Dessau, Z.X. Shen, B.O. Wells, D.M. King, W.E. Spicer, A.J. Arko, L.W. Lombardo, D.B. Mitzi, and A. Kapitulnik, Phys. Rev. B **45**, 5095 (1992).

[10] P.B. Littlewood and C.M. Varma, Phys. Rev. B **46**, 405 (1992).

[11] J.C. Campuzano, H. Ding, M.R. Norman, H.M. Fretwell, M. Randeria, A. Kaminski, J. Mesot, T. Takeuchi, T. Sato, T. Yokoya, T. Takahashi, T. Mochiku, K. Kadowaki, P. Guptasarma, D.G. Hinks, Z. Konstantinovic, Z.Z. Li, and H. Raffy, Phys. Rev. Lett. **83**, 3709 (1999).

[12] Y.-D. Chuang, A.D. Gromko, A. Fedorov, Y. Aiura, K. Oka, Yoichi Ando, H. Eisaki, S.I. Uchida, and D.S. Dessau, Phys. Rev. Lett. **87**, 117002 (2001).

[13] Y.-D. Chuang, A.D. Gromko, A.V. Fedorov, Y. Aiura, K. Oka, Yoichi Ando, and D.S. Dessau, cond-mat/0107002 (unpublished).

[14] D.L. Feng, N.P. Armitage, D.H. Lu, A. Damascelli, J.P. Hu, P. Bogdanov, A. Lanzara, F. Ronning, K.M. Shen, H. Eisaki, C. Kim, Z.-X. Shen, J.-i. Shimoyama, and K. Kishio, Phys. Rev. Lett. **86**, 5550 (2001).

[15] S.V. Borisenko, A.A. Kordyuk, T.K. Kim, S. Legner, K.A. Nenkov, M. Knupfer, M.S. Golden, J. Fink, H. Berger, and R. Follath, Phys. Rev. B **66**, 140509(R) (2002); A.A. Kordyuk, S.V. Borisenko, T.K. Kim, K.A. Nenkov, M. Knupfer, J. Fink, M.S. Golden, H. Berger, and R. Follath, Phys. Rev. Lett. **89**, 077003 (2002).

[16] A. Kaminski, S. Rosenkranz, H.M. Fretwell, Z. Li, H. Raffy, M. Randeria, M.R. Norman, and J.C. Campuzano, Phys. Rev. Lett. **90**, 207003 (2003).

[17] T. Valla, A.V. Fedorov, P.D. Johnson, B.O. Wells, S.L. Hulbert, Q. Li, G.D. Gu, and N. Koshizuka, Science **285**, 2110 (1999).

[18] A Lorentzian approximates the B band MDC line shape fairly closely, implying that the self-energy varies minimally over the $\vec{k}$ width ($\sim 0.1\pi$) of the peak.

[19] A Lorentzian on a linear background was multiplied by a Fermi function.

[20] M.R. Norman, H. Ding, J.C. Campuzano, T. Takeuchi, M. Randeria, T. Yokoya, T. Takahashi, T. Mochiku, and K. Kadowaki, Phys. Rev. Lett. **79**, 3506 (1997); Phys. Rev. B **57**, R11 089 (1998).

[21] C.G. Olson, R. Liu, D.W. Lynch, R.S. List, A.J. Arko, B.W. Veal, Y.C. Chang, P.Z. Jiang, and A.P. Paulikas, Phys. Rev. B **42**, 381 (1990).

[22] A.D. Gromko, Y.-D. Chuang, A.V. Fedorov, Y. Aiura, Y. Yamaguchi, K. Oka, Yoichi Ando, and D.S. Dessau, cond-mat/0205385 (unpublished).

[23] P.B. Littlewood and C.M. Varma, Phys. Rev. B **46**, 405 (1992).

[24] P. Bourges, in *The Gap Symmetry and Fluctuations in High Temperature Superconductors*, edited by J. Bok, G. Deutscher, and D. Pavuna (Plenum Press, Cambridge, 1998).

[25] H.F. Fong, P. Bourges, Y. Sidis, L.P. Regnault, A. Ivanov, G.D. Gu, N. Koshizuka, and B. Keimer, Nature (London) **398**, 588 (1999).

[26] Pengcheng Dai, H.A. Mook, S.M. Hayden, G. Aeppli, T.G. Perring, R.D. Hunt, and F. Dogan, Science **284**, 1344 (1999).

[27] S.V. Borisenko, A.A. Kordyuk, T.K. Kim, A. Koitzsch, M. Knupfer, J. Fink, M.S. Golden, M. Eschrig, H. Berger, and R. Follath, Phys. Rev. Lett. **90**, 207001 (2003).

[28] H. He, Y. Sidis, P. Bourges, G.D. Gu, A. Ivanov, N. Koshizuka, B. Liang, C.T. Lin, L.P. Regnault, E. Schoenherr, and B. Keimer, Phys. Rev. Lett. **86**, 1610 (2001).

[29] H.A. Mook, Pengcheng Dai, S.M. Hayden, G. Aeppli, T.G. Perring, and F. Dogan, Nature (London) **580**, 580 (1998).

[30] L.B. Ioffe and A.J. Millis, Phys. Rev. B **58**, 11 631 (1998).

[31] Z.-X. Shen and J.R. Shrieffer, Phys. Rev. Lett. **78**, 1771 (1997).

[32] A. Abanov, A.V. Chubukov, and J. Schmalian, J. Electron Spectrosc. Relat. Phenom. **117-118**, 129 (2000).

[33] E. Demler and S.-C. Zhang, Phys. Rev. Lett. **75**, 4126 (1995).

[34] M. Eschrig and M.R. Norman, Phys. Rev. Lett. **89**, 277005 (2002).

[35] S.-C. Zhang (private communication).

[36] T.K. Kim, A.A. Kordyuk, S.V. Borisenko, A. Koitzsch, M. Knupfer, H. Berger, and J. Fink, cond-mat/0303422 (unpublished).